Eur Spine J (2006) 15: 1845–1851
DOI 10.1007/s00586-005-0035-2

ORIGINAL ARTICLE

Giuseppe Longo
Purificacion Ripalda
Vicenzo Denaro
Francisco Forriol

# Morphologic comparison of cervical, thoracic, lumbar intervertebral discs of cynomolgus monkey (*Macaca fascicularis*)

Received: 18 January 2005
Revised: 15 June 2005
Accepted: 30 November 2005
Published online: 23 December 2005


P. Ripalda · F. Forriol (✉)
Orthopaedic Surgery and Traumatology,
University of Navarra, Pamplona,
Navarra, Spain
E-mail: fforriol@gmail.com
Tel.: +34-948-255400
Fax: +34-948-425649

G. Longo · V. Denaro
Orthopaedic Department,
Universita Campus BioMedico,
Rome, Italy

*Present address*: F. Forriol
Valle de Laciana 82,
28034 Madrid, Spain

**Abstract** The aim was to analyze the morphological differences of the intervertebral disc and endplates at different levels. Forty-five vertebral motion segments were obtained from the spine of nine 3 to 4-year-old cynomolgus monkeys (*Macaca fascicularis*). From every spine, five discs were sectioned (C5–C6, T3–T4, T9–T10, L2–L3, L4–L5). In all the groups, tissue samples were collected and sections were stained with Masson's trichrome, Safranine-O and van Gieson's connective tissue stain to analyze the intervertebral discs. Immunohistochemistry was performed, using specific antibodies to detect collagens I and II. The intervertebral disc height, the maximum nucleus pulposus height, the superior and inferior endplate heights were histomorphometrically measured and different indexes were calculated to compare the differences between specimens of the same animal and between discs of the same level, and finally the differences between groups of discs of different levels. There were no differences existing in annular fibers anchoring on the endplate between discs of different levels. A positive immune reaction for type I collagen was observed in the longitudinal ligaments and in the annular region adjacent to them. Collagen II immune reactivity was found in the annulus close to the nucleus pulposus, in the endplates and in the nucleus. There were no differences between discs of different levels in the collagen I and II localization. The height of the discs varied along the spine. The smallest value was measured in T3–T4, with a larger increase caudally than cranially. The highest value was measured in L2–L3. A cervical disc was 55% the height of a lumbar one. The endplate height increased along the length of the spine. The inferior EP was always higher than the superior. The study provides a detailed structural characterization of the intervertebral disc and may be useful for further investigations on the disc degeneration process.

**Keywords** Intervertebral disc · Endplate · Nucleus pulposus · Annulus fibrosus · *Macaca fascicularis*

## Introduction

The intervertebral disc (IVD) is a complex structure composed of various connective tissues, which undergoes biochemical and structural changes with aging. IVD pathology is very frequent [7, 13] and causes high health care costs in Western industrialized countries [5, 7]. Despite the importance of the problem, causes and mechanisms of disc degeneration are not fully understood. One factor which contributes to the pathogenesis of degenerative disc disease is microavulsions of the attachment of the annulus fibrosus (AF) at the endplate (EP). These may constitute a pathogenic precursor to the actual degenerative disc disease process [11].

Furthermore, disc pathology is different according to the place in the spine. In fact, while disc prolapse is common in the lumbar spine, degenerative disc changes in the cervical spine are described as thinning and collapse of the disc, endplate sclerosis, bulging annulus fibrosus, osteophyte formation on joints and on the vertebral body margins, chondro-osseous spur formation which narrows the spinal canal or intervertebral foramina [6, 8, 22, 25].

Moreover, symptomatic thoracic disc disease is less common than cervical or lumbar disease [31]. A key role in limiting thoracic spine movements is played from the ribs. If on the one hand the costovertebral joints increase the stability of whole spine, on the other they reduce the thoracic segment mobility [2, 15]. Furthermore the small size of the thoracic IVDs is itself a movement-limiting factor [9, 15].

The reason why the spine pathology is not the same in the different spine regions could be that IVDs are structurally different in the different spine areas [22, 24] due to the fact that they are subjected to different mechanical stresses and load bearing.

The aim of this study was to analyze the morphological differences of the IVD at different levels focusing on the endplate and the anchorage of the disc fibers to the vertebrae and the distribution pattern of collagens I and II in adult cynomolgus monkeys (*Macaca fascicularis*). In order to compare the IVDs of different spine levels, we chose the monkey because, though a quadruped, it is an animal that sometimes assumes erected position. In such way, the stresses that its discs receive are more similar to those which human discs receive in comparison with all other animals [19, 20].

## Materials and methods

Forty-five vertebral motion segments were obtained from the spine of nine 3 to 4-year-old adult male cynomolgus monkeys (*M. fascicularis*), weighing from 2.5 to 3 kg.

The monkeys were anesthetized with sodium pentobarbital (1 mg/kg) and killed with KCl (5 meq). The entire spine was excised, freed from soft tissue, frozen and stored at −20°C.

From every spine five vertebral motion segments were later sectioned (C5–C6, T3–T4, T9–T10, L2–L3, L4–L5) and cut in half by a medial sagittal cut.

The study had the approval of the Deontological Committee for Animal Experimentation of our University and followed the current regulations, which were in accord with the Stockholm Meeting on experimentation with animals.

### Histology

In all the groups, tissue samples were collected from the IVDs. Once fixed with buffered formaldehyde at 4%, the pieces were decalcified (EDTA–PVP) and dehydrated, embedded in paraffin and cut into 4 μm sections. Finally, sections were stained with Masson's trichrome, Safranine-O, which reflects the amount of proteoglycans present in the sample, and van Gieson's connective tissue stain for elastic fibers and examined using conventional and polarized light microscopy.

On specimens obtained by means of mid-sagittal cuts of the movement segment, we researched differences in the annular fibers' anchorage to the vertebra between the annular region ringing the nucleus pulposus (NP) and the annular region adjacent to the longitudinal ligaments (LLs) at all levels.

In order to determine structural differences between cervical, thoracic and lumbar IVDs, we compared first the differences between specimens of the same animal, then the differences between discs of the same level and finally the differences between groups of discs of different levels.

### Immunohistochemistry

Immunohistochemistry was performed using specific antibodies to detect collagens I and II. The sections were dewaxed in xylene and taken through ethanol 100%. Endogenous peroxidase activity was blocked by immersion in hydrogen peroxide (3%) in methanol, for 30 min, at room temperature in darkness. The sections were hydrated using alcohols of decreasing proof (100, 96, 80 and 70%). The antibodies that were required were introduced in trypsin 0.1%. Then the sections were washed in TBS (tris–HCl 0.05 M, NaCl 0.5 M, pH 7.36) and incubated in normal porcine serum at a dilution of 1:20, for 30 min, in a humid chamber at room temperature. The pieces were incubated with the respective antibodies, at 4°C overnight, then incubated with secondary antibodies (30 min 1:200) and then with avidine–biotine complex unit to peroxidase (K0355 Dako®), for 30 min, at room temperature and a dilution of 1:100.The slices were then treated with a visualization solution containing 3,3′-diaminobencidine tetrahydrochloride (Sigma-Aldrich®) 0.3 mg/ml with 0.005% $H_2O_2$ in TB (tris–HCl 0.05 M, pH 7.36). They were counterstained with Harris hematoxylin, dehydrated and finally mounted in DPX. As a negative control, we followed the same process, but replacing the antibodies with TBS.

The collagen I antibody was a rabbit polyclonal immunoglobulin G used at a dilution of 1:50 (2150-0020 Biogenesis®). The collagen I antibody was placed in trypsin 0.1% for 1 h.

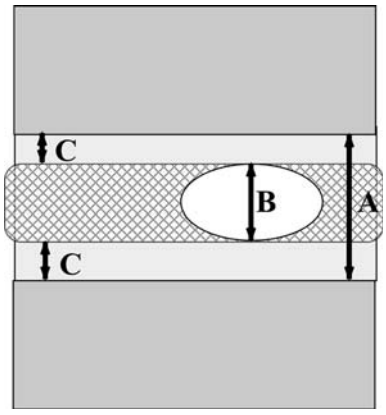


**Fig. 1** The intervertebral disc height (A), the maximum nucleus pulposus height (B), the superior and inferior endplate heights (C and D)

The collagen II antibody was a rabbit polyclonal immunoglobulin G used at a dilution of 1:50 (2150-0060 Biogenesis®). The collagen II antibody was placed in trypsin 0.1% for 1 h and 30 min.

### Histomorphometry

The Safranine-O and Masson's trichrome specimens obtained by means of mid-sagittal sections were measured using a microscope with an image analysis system (Leica Q 500 MC®, Cambridge, UK). We analyzed the IVD and the superior and inferior EPs. Measurements were performed in all groups, in three serial slices and in five fields per slice.

The IVD height had a medium value of 500 measured with the imagine analyzer of three series cuts between the superior and inferior EP limits. The same method was utilized to obtain the superior and inferior EP height. The maximum NP height was the maximum height value obtained in the NP in three serial slices.

The following measurements were taken: the IVD height (IVDH), the maximum NP height (mNPH), the superior and inferior EP heights (SEPH and IEPH). Then the average of every disc group was compared with the average of the corresponding IVDH (Fig. 1).

With the parameters obtained we calculated different ratios, such as the EP/IVDH index, NP/IVDH index, SEPH/IEPH index and the superior and inferior EPH percentages.

## Results

The central NP portion was always, at all levels, in direct contact with the EPs, whereas the peripheral regions did

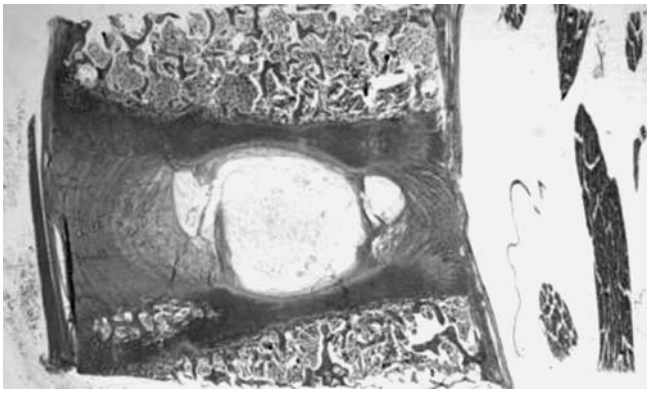

**Fig. 2** The central nucleus pulposus portion was always in direct contact with the endplates, whereas the peripheral regions did not directly touch them (Safranine-O, ×0.5)

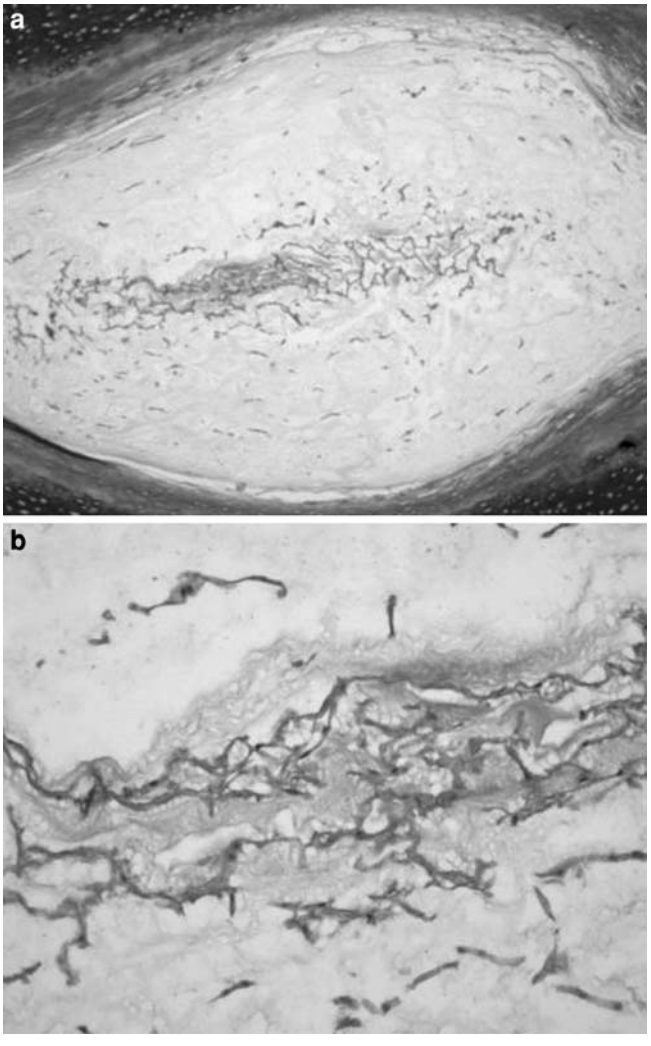


**Fig. 3** The monkey nucleus pulposus showed scattered fibroblast-like cells, surrounded by large zones of acellular matrix: **a** Masson's trichrome, ×4; **b** Masson's trichrome, ×10

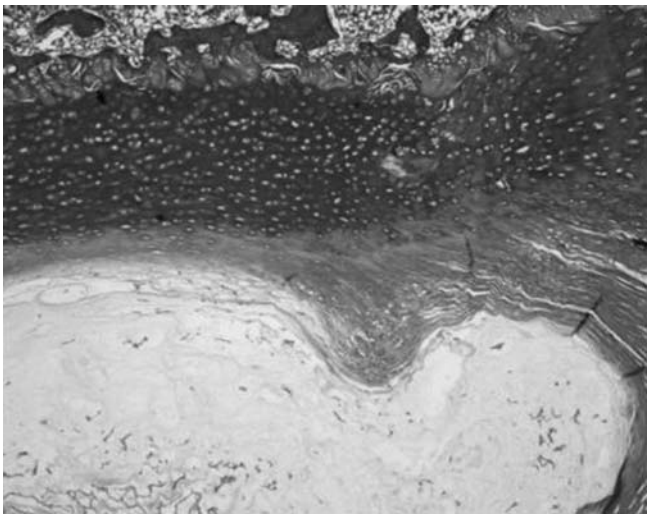

**Fig. 4** The fibrocartilage in the monkey nucleus pulposus was present as fibers which, though invading the nucleus pulposus, did not divide it (Masson's trichrome, ×4)

not have direct contact with them (Fig. 2). Masson's trichrome staining showed scattered fibroblast-like cells, surrounded by large zones of acellular matrix (Fig. 3). The polarized light microscopy permitted us to distinguish NP with and without fibrocartilage. These findings were confirmed from the immunoreactivity to collagen I.

The fibrocartilage in the NP was present in the form of fibers which, though invading the NP, did not divide it (Fig. 4) or as fibers that united the two EPs and divided the NP. The fibrocartilage presented fibroblast-like cells and elongated chondrocyte-like cells scattered in the direction of the fibers. Fibrocartilage invading the NP without dividing it was observed in cervical and thoracic IVDs, whereas in lumbar discs fibrocartilage invading the NP and dividing it was present. Immunoreactivity to collagen II was found in the NP, but not to collagen I.

The EP was formed by three zones: a cartilaginous zone adjacent to the NP, an intermediate zone of cartilage with areas of mineralization and a zone adjacent to the vertebral body, consisting of growth cartilage (Fig. 5). We noticed that the cartilaginous zone ended where NP finished.

Annular fibers adjacent to the NP penetrated and anchored to this endplate zone (Fig. 6). Chondrocytes were elongated in the direction of the fibers. The number of cells seemed to depend on the disc's conditions, more than on the spinal position. In fact IVDs with a very mineralized EP and a fibrocartilaginous NP had only a small number of cells in the cartilaginous zone.

We found areas of mineralization in the intermediate zone of the EP and saw chondrocytes in the surrounding cartilage, but not in the areas of mineralization.

A mineralized tidemark line was well evident in the transition between annular fibers adjacent to LLs and mineralized endplate zone, but not between the annular fibers adjacent to the NP and the non-mineralized cartilaginous zone. This mineralized tidemark line was not in continuity with the mineralization areas of the EP. Mineral deposition stripes from the mineralized cartilaginous endplate zone followed the initial portion of fibers of the annular fibers adjacent to LLs and of the fibers continuing in the LLs (Fig. 7). In all pieces we found annular fibers adjacent to the LLs and fibers continuing in the LLs anchoring to the mineralized endplate zone (Fig. 8).

The cartilaginous mineralized zone was always the largest, in all the sections we analyzed. Nine lumbar

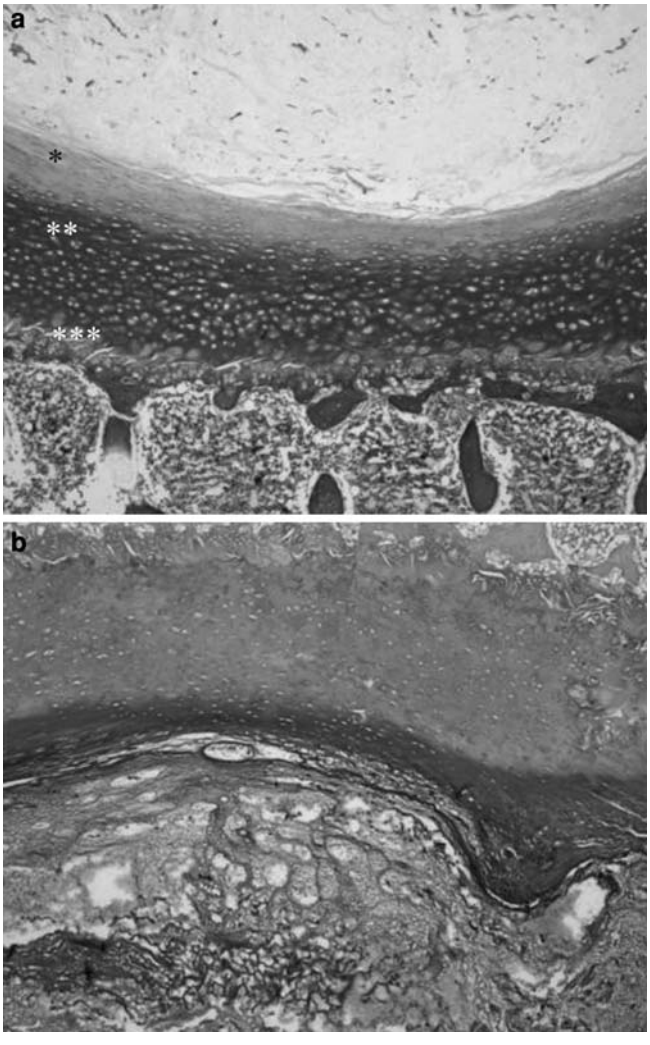


**Fig. 5** The monkey endplate was formed by three zones: a cartilaginous zone adjacent to the nucleus pulposus (*), an intermediate zone of cartilage with areas of mineralization (**) and a zone adjacent to the vertebral body (***), made up of growth cartilage; **a** Masson's trichrome, ×4; **b** Safranine-O, ×4

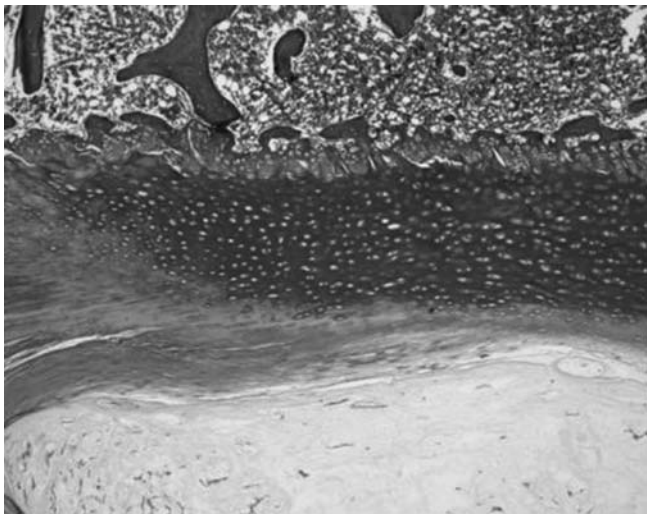

**Fig. 6** Annular fibers adjacent to the nucleus pulposus penetrated and anchored to the cartilaginous zone adjacent to the nucleus pulposus (Masson's trichrome, ×4)

IVDs (five L4–L5 and four L2–L3) presented large ossification regions in the EP.

The zone adjacent to the vertebral body was made of growth cartilage, with hypertrophic chondrocytes organized in irregular columns. Scattered ossification gaps invaded this zone. The growth cartilage zone was in contact with the cancellous vertebral bone. Immune reactivity to collagen II was found in the EP, but there was no immune reactivity to collagen I.

There were no differences existing in annular fibers anchoring to the EP among discs of different levels. In the fibrocartilage tissue of the AF, chondrocyte-like cells and fibroblast-like cells were scattered between the bundles of the fibers. Van Gieson's connective tissue stain for elastic fibers showed, in the lumbar discs, transversal bundles that did not show immune reactivity to collagens I and II.

A positive immune reaction for type I collagen, but not for collagen II, was observed in the LLs and in the annular region adjacent to them. The collagen I staining was wider anteriorly than posteriorly. Collagen II immune reactivity was found in the annular region close to the NP.

The height of the IVD varied along the length of the spine (Table 1). The smallest value was measured in T3–T4, with a larger increase caudally than cranially. The highest value was measured in L2–L3. A cervical IVD was 55% the height of a lumbar one.

The superior/inferior EP height indexes were similar (Table 2). The EP percentages of L2–L3 with respect to IVDH were the smallest, although the L2–L3 discs were the highest. The EP height increased along the length of the spine. The inferior EP was always higher than the superior (Table 2).

## Discussion

The present study provides an exhaustive description of the histological and immunohistochemical architecture of the IVD of *M. fascicularis* and shows that the IVD of *M. fascicularis* is very similar to human IVD in that regard. In fact the EP of *M. fascicularis* has an analogous structure to the human one [3, 4] and, like in humans, NP and EP are immunoreactive to collagen II while the region of the annulus adjacent to the LLs is immunoreactive to collagen I [7, 21, 23, 27, 29].

Several collagen types are present in the IVD [1, 21, 23, 27] and they form a fibrous network that holds cells

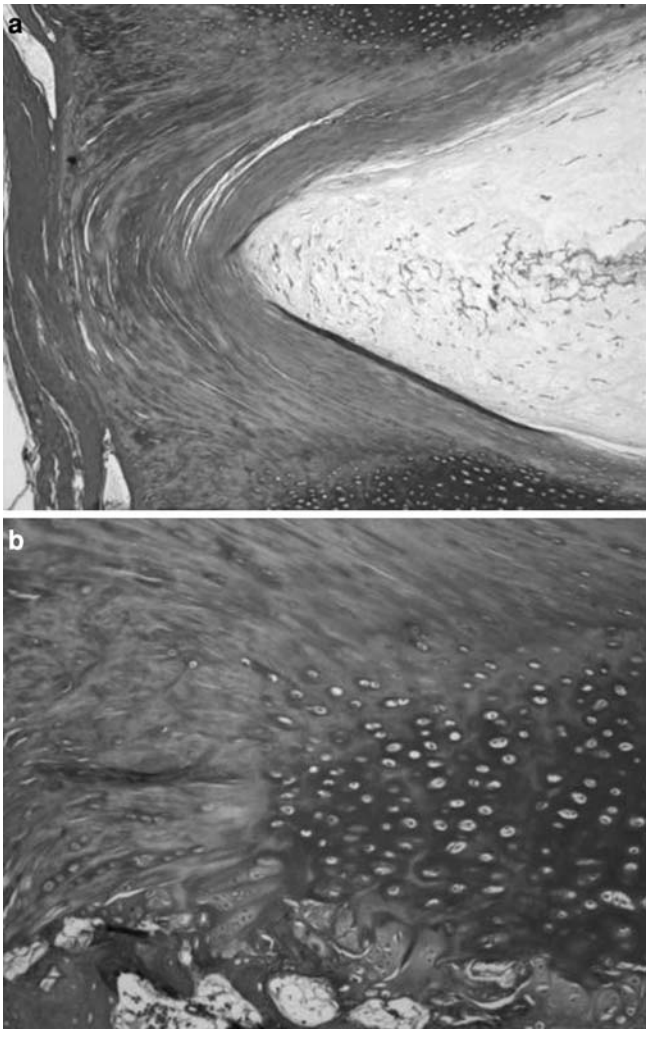


**Fig. 7** Annular fibers adjacent to the longitudinal ligaments anchored to the mineralized cartilaginous endplate zone. A mineralized tidemark line delimited the lateral portions of the mineralized endplate zone. Mineral deposition stripes from the mineralized cartilaginous endplate zone followed the initial portion of fibers of the annular fibers adjacent to longitudinal ligaments and of the fibers continuing in the longitudinal ligaments. Numerous oval chondrocytes were present between the mineral deposition stripes; **a** Masson's trichrome, ×4; **b** Masson's trichrome, ×10

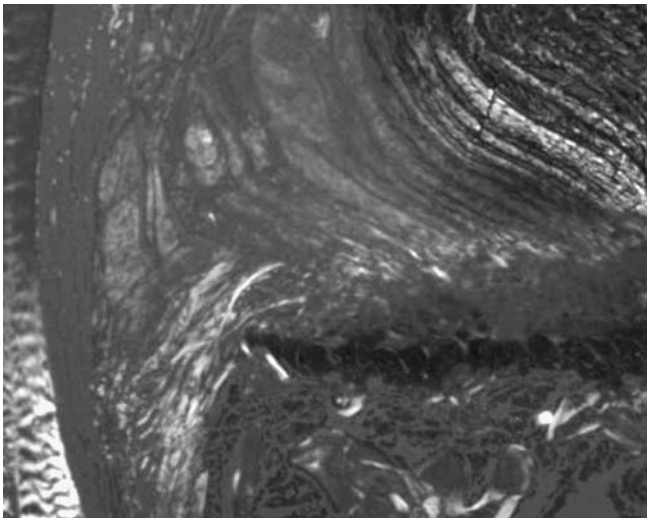

**Fig. 8** Polarized microscopy showed the annular fibers adjacent to the longitudinal ligaments and the fibers continuing in the longitudinal ligaments anchoring to the mineralized endplate zone (×4)

and proteoglycans in the matrix [5]. Fibrillar collagens I and II are the most important collagen types (80% of the collagen in the IVD is made up of fibrillar collagens) [1, 7, 27]. We found immune reactivity to collagen I in the region of the annulus adjacent to the *LLs*, as previously demonstrated in humans [7, 23, 24, 28, 30]. These structural features supply this portion of the IVD with the characteristic to withstand tension stresses [16, 19].

The NP and EP in *M. fascicularis* were immunoreactive to collagen II, like in humans [7, 21, 23, 27, 29], which is typical of articular cartilage and which supplies this portion of the IVD with the ability to withstand compressive stresses [14, 15, 17].

Fibrous tissue is adapted to withstand tension stresses rather than compressive stresses, but in the lordotic lumbar spine, gravitational compression falls most heavily on the posterior components of the IVD [15]. Furthermore, we found the annular fibers adjacent to the LLs to be much less numerous posteriorly. For these reasons the posterior part of the AF is a site of potential weakness [15, 30].

**Table 2** Nucleus pulposus, superior and inferior endplate height indexes (percentage)

| Level | NP/DH (%) | SEP/DH (%) | IEP/DH (%) | SEP/IEP (%) | (SEP + IEP)/DH (%) |
|---|---|---|---|---|---|
| C5–C6 | 27 | 21 | 22 | 0.92 | 43 |
| T3–T4 | 28 | 22 | 23 | 0.94 | 45 |
| T9–T10 | 34 | 17 | 18 | 0.93 | 35 |
| L2–L3 | 28 | 15 | 17 | 0.87 | 32 |
| L4–L5 | 34 | 19 | 21 | 0.90 | 40 |

*DH* disc height, *NP* nucleus pulposus, *SEP* superior endplate, *IEP* inferior endplate

Like Roberts et al. [27], we did not find any difference in the immunolocalization of collagens I and II among the discs of different levels.

The fibers of the region of the annulus adjacent to the NP anchor to the cartilaginous EP and our findings are in accordance with those of Inoue [18]. But, while several authors [16–18] describe the annulus fibers of the region adjacent to the LLs anchoring to the bony vertebral body, we saw these fibers anchor to the second mineralized layer of the EP, as did Francois [12].

The EP is made up of three regions, as in humans [3, 4]. The nutrition of the disc, the largest avascular tissue in the body [15, 17] with the exception of the outer third of the AF [13], depends on the diffusion of nutrients through the EP and through the outer annulus. EP calcifications can determine important variations of the nutrition of the disc [4]. It has been suggested that calcification of the cartilage EP may play an important role in pathologies like scoliosis and be highly significant to the progression of the scoliotic curve [26, 28].

We did not find a well-delimited cortical bone at the interface between the EP and the vertebral bone, but several bone marrow contacts, through which the IVD receives nutrients [15, 17, 18].

We found in *M. fascicularis* that the smallest discs are the T3–T4 and C5–C6. Superior and inferior EP heights increased cranio-caudally, and we measured the higher values in lumbar discs, as in human spine [24].

The results of this study provide a detailed structural characterization of the IVD of *M. fascicularis* and may be helpful in the evaluation of this animal model for research into the IVD.

**Table 1** Intervertebral disc, maximum nucleus pulposus, superior and inferior endplate heights (mm)

| Disc level | Intervertebral disc height | | Maximum nucleus pulposus height | | Superior endplate height | | Inferior endplate height | |
|---|---|---|---|---|---|---|---|---|
| | Mean | SD | Mean | SD | Mean | SD | Mean | SD |
| C5–C6 | 2.93 | 0.11 | 0.78 | 0.14 | 0.61 | 0.03 | 0.65 | 0.02 |
| T3–T4 | 2.88 | 0.1 | 0.79 | 0.11 | 0.62 | 0.09 | 0.66 | 0.09 |
| T9–T10 | 3.99 | 0.66 | 1.34 | 0.13 | 0.68 | 0.02 | 0.73 | 0.04 |
| L2–L3 | 5.33 | 0.40 | 1.48 | 0.26 | 0.79 | 0.12 | 0.91 | 0.148 |
| L4–L5 | 5.01 | 0.77 | 1.68 | 0.24 | 0.95 | 0.07 | 1.05 | 0.04 |

## References


1. Alini M, Roughley PJ, Antoniou J, Stoll T, Aebi M (2002) A biological approach to treating disc degeneration: not for today, but maybe for tomorrow. Eur Spine J 11:S215–S220
2. Benzel EC (1995) Biomechanics of spine stabilization: principles and clinical practice. McGraw-Hill, New York
3. Benneker LM, Heini PF, Alini M, Anderson SE, Ito K (2005) 2004 Young award winner: vertebral endplate marrow contact channel occlusions and intervertebral disc degeneration. Spine 15(30):167–173
4. Bernick S, Cailliet R (1982) Vertebral end-plate changes with aging of human vertebrae. Spine 2:97–102
5. Bibby SR, Jones DA, Lee RB, Yu J, Urban JPG (2001) The pathophysiology of the intervertebral disc. Joint Bone Spine 6:537–542
6. Boni M, Denaro V (1987) Anatomoclinical correlations in cervical spondylosis. Springer, Berlin Heidelberg New York, pp 3–20
7. Cassinelli EH, Hall RA, Kang JD (2001) Biochemistry of intervertebral disc degeneration and the potential for gene therapy applications. Spine J 3:205–214
8. Denaro V (1991) Stenosis of the cervical spine. Springer, Berlin Heidelberg New York
9. De Palma AF, Rothman RH (1970) The intervertebral disc. WB Saunders, Philadelphia
10. Eurell JA, Kazarian LE (1986) The vertebral cartilaginous endplate of the preadult rhesus monkey (*Macaca mulatta*). A correlative scanning electron- and light-microscopic study. Spine 5:483–486
11. Fornasier VL, Garaffo G, Denaro L, Denaro V (2000) Intervertebral disc degeneration—an autopsy study. Eur J Orthop Surg Traumatol 10:159–165
12. Francois RJ (1982) Three-dimensional architecture of lumbar intervertebral discs. Spine 5:522–523
13. Freemont AJ, Watkins A, Le Maitre C, Jeziorska M, Hoyland JA (2002) Current understanding of cellular and molecular events in intervertebral disc degeneration: implications for therapy. J Pathol 4:374–379
14. Ganey TM, Meisel HJ (2002) A potential role for cell-based therapeutics in the treatment of intervertebral disc herniation. Eur Spine J Suppl 2:S206–S214
15. Grieve P (1988) Common vertebral joint problems. Churchill Livingstone, London
16. Hashizume H (1980) Three-dimensional architecture and development of lumbar intervertebral discs. Acta Med Okayama 34:301–314
17. Humzah MD, Soames RW (1988) Review. Human intervertebral disc: structure and function. Anat Rec 4:337–356
18. Inoue H (1981) Three-dimensional architecture of lumbar intervertebral discs. Spine 2:139–146
19. Luk KD, Ruan DK, Chow DH, Leong JC (1997) Intervertebral disc autografting in a bipedal animal model. Clin Orthop 337:13–26
20. Luk KD, Ruan DK, Lu DS, Fei ZQ (2003) Fresh frozen intervertebral disc allografting in a bipedal animal model. Spine 28:864–869
21. Mercer S, Bogduk N (1999) The ligaments and annulus fibrosus of human adult cervical intervertebral discs. Spine 7:619–626
22. Nerlich AG, Schleicher ED, Boos N (1997) 1997 Volvo award winner in basic science studies. Immunohistologic markers for age-related changes of human lumbar intervertebral discs. Spine 24:2781–2795
23. Nerlich AG, Boos N, Wiest I, Aebi M (1998) Immunolocalization of major interstitial collagen types in human lumbar intervertebral discs of various ages. Virchows Arch 1:67–76
24. Pooni JS, Hukins DW, Harris PF, Hilton RC, Davies KE (1986) Comparison of the structure of human intervertebral discs in the cervical, thoracic and lumbar regions of the spine. Surg Radiol Anat 3:175–182
25. Prescher A (1998) Anatomy and pathology of the aging spine. Eur J Radiol 27:181–195
26. Roberts S, Menage J, Urban JP (1989) Biochemical and structural properties of the cartilage end-plate and its relation to the intervertebral disc. Spine 2:166–174
27. Roberts S, Menage J, Duance V, Wotton S, Ayad S (1991) 1991 Volvo award in basic sciences. Collagen types around the cells of the intervertebral disc and cartilage end plate: an immunolocalization study. Spine 9:1030–1038
28. Roberts S, Menage J, Eisenstein SM (1993) The cartilage end-plate and intervertebral disc in scoliosis: calcification and other sequelae. J Orthop Res 5:747–757
29. Schollmeier G, Lahr-Eigen R, Lewandrowski KU (2000) Observations on fiber-forming collagens in the anulus fibrosus. Spine 21:2736–2741
30. Tsuji H, Hirano N, Ohshima H, Ishihara H, Terahata N, Motoe T (1993) Structural variation of the anterior and posterior anulus fibrosus in the development of human lumbar intervertebral disc. A risk factor for intervertebral disc rupture. Spine 2:204–210
31. Vanichkachorn JS, Vaccaro AR (2000) Thoracic disk disease: diagnosis and treatment. J Am Acad Orthop Surg 3:159–69